A mutation in mouse *Disc1* that models a schizophrenia risk allele leads to specific alterations in neuronal architecture and cognition

Mirna Kvajo*[†], Heather McKellar[‡], P. Alexander Arguello[§], Liam J. Drew[†], Holly Moore*, Amy B. MacDermott[†§], Maria Karayiorgou*[¶], and Joseph A. Gogos[†§¶]

Departments of *Psychiatry and [§]Neuroscience, Columbia University Medical Center, 1051 Riverside Drive, New York, NY 10032; [†]Department of Physiology and Cellular Biophysics, Columbia University Medical Center, 630 West 168th Street, New York, NY 10032; and [‡]Integrated Program in Cellular, Molecular, and Biophysical Studies, Columbia University, New York, NY 10032

Communicated by Gerald D. Fischbach, Columbia University College of Physicians and Surgeons, New York, NY, March 18, 2008 (received for review November 8, 2007)

***DISC1* is a strong candidate susceptibility gene for schizophrenia, bipolar disorder, and depression. Using a mouse strain carrying an endogenous *Disc1* orthologue engineered to model the putative effects of the disease-associated chromosomal translocation we demonstrate that impaired *Disc1* function results in region-specific morphological alterations, including alterations in the organization of newly born and mature neurons of the dentate gyrus. Field recordings at CA3/CA1 synapses revealed a deficit in short-term plasticity. Using a battery of cognitive tests we found a selective impairment in working memory (WM), which may relate to deficits in WM and executive function observed in individuals with schizophrenia. Our results implicate malfunction of neural circuits within the hippocampus and medial prefrontal cortex and selective deficits in WM as contributing to the genetic risk conferred by this gene.**

bipolar disorder | gene | mouse model | working memory | adult neurogenesis

A balanced chromosomal translocation segregating with schizophrenia and affective disorders in a large Scottish family (1) implicated *DISC1* as a susceptibility gene for major mental illness. Additional support for this gene was provided by the observation that mice engineered to carry a truncating lesion in the endogenous *DISC1* orthologue have deficits in working memory (WM) (2), a well established schizophrenia endophenotype (3). Common variation in *DISC1* may also play a role in psychiatric disorders in karyotypically normal patient populations (4), indicating that *DISC1*, especially the well defined risk allele found in the Scottish pedigree, represents a potentially valuable tool for gaining insight into the pathogenesis of mental illnesses.

The function of *DISC1* is at present poorly understood. Its potential association with cytoskeletal and centrosomal proteins and phosphodiesterase 4b (PDE4B), suggests involvement in cell migration, neurite outgrowth, and cAMP signaling (5–7). However, it is not known which of these interactions are relevant in understanding the contribution of the gene to psychiatric disorders. Several mouse models generated to investigate *Disc1* function have been reported and shown to display diverse profiles of behavioral and cellular abnormalities (8–11). Models overexpressing truncated versions of human DISC1 protein under various exogenous promoters either constitutively (8) or transiently during early postnatal life (11) provided preliminary evidence for irreversible effects of transient postnatal impairment of *Disc1*, whereas those carrying *N*-ethyl-*N*-nitrosourea-induced mutations in the *Disc1* gene (9) demonstrated that allelic heterogeneity at the *DISC1* locus can lead to distinct behavioral phenotypes.

We used an alternative, disease-oriented approach (3, 12, 13) to generate mutant mice carrying a truncating lesion in the endogenous *Disc1* orthologue that models the only well defined *DISC1* schizophrenia risk allele (2). This approach preserves the endogenous spatial and temporal expression pattern of the gene, thus preventing the induction of neomorphic phenotypic features. A comprehensive analysis of these mice implicates malfunction of neural circuits within the hippocampus (HPC) and medial prefrontal cortex (mPFC), and selective deficits in WM as contributing to the genetic risk conferred by the *DISC1* gene.

Results

The mutant mouse strain used in this study propagates a *Disc1* allele (Mouse Genome Informatics nomenclature: $Disc1^{Tm1Kara}$) (Fig. 1*A*) that carries two termination codons (in exons 7 and 8) and a premature polyadenylation site in intron 8, which leads to the production of a truncated transcript (2). Western blot analysis of total brain extracts around the peak of postnatal *Disc1* expression using two polyclonal antibodies raised against N-terminal (2) and C-terminal [see supporting information (SI) Fig. S1 *A* and *B*] Disc1 protein moieties revealed that the introduced genetic lesion results in the elimination of the major isoforms of Disc1 at ≈98-kDa (predicted full-length proteins L and L_v forms http://genome.ucsc.edu) and ≈70 kDa (14). It also results in the production of low levels of a predicted truncated protein product detected, as expected, by the N-terminal but not the C-terminal antibody (Fig. 1*B*). In the adult brain, Disc1 levels are drastically reduced (15). In the adult HPC, the ≈70-kDa signal is undetectable, although a WT-specific signal still persists at the 98-kDa range (L and L_v forms). No truncated protein product is observed (Fig. 1*B*). It should be noted that two commercially available antibodies raised against small peptide epitopes located at the N and C terminal of Disc1 failed to detect elimination of specific WT bands, both at the 98- and 70-kDa range. Moreover, the N-terminal peptide antibody failed to recognize the novel product at the expected size of a truncated Disc1 protein (Fig. S1 *C* and *D*). Thus, unlike two polyclonal antibodies raised against extended protein domains, both peptide antibodies demonstrate lack of specificity when used to analyze complex brain extracts, raising questions about the

Author contributions: M. Kvajo, H. McKellar, and P.A.A. contributed equally to this work; M. Kvajo, H. McKellar, P.A.A., M. Karayiorgou, and J.A.G. designed research; M. Kvajo, H. McKellar, P.A.A., and L.J.D. performed research; H. Moore and A.B.M contributed new reagents/analytic tools; M. Kvajo, H. McKellar, P.A.A., L.J.D., H. Moore, and A.B.M. analyzed data; and M. Kvajo, H. McKellar, P.A.A., M. Karayiorgou, and J.A.G. wrote the paper.

The authors declare no conflict of interest.

Freely available online through the PNAS open access option.

[¶]To whom correspondence may be addressed. E-mail: mk2758@columbia.edu or jag90@columbia.edu.

This article contains supporting information online at www.pnas.org/cgi/content/full/0802615105/DCSupplemental.

© 2008 by The National Academy of Sciences of the USA

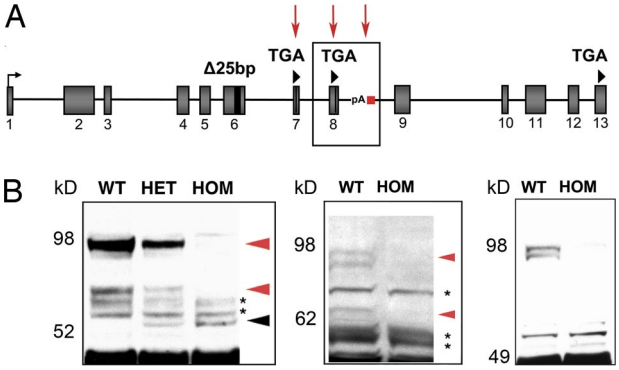

Fig. 1. Structure of the targeted *Disc1* allele and its consequences on protein production and brain morphology. (*A*) A multiply compromised *Disc1* allele. The modified *Disc1* allele carries (*i*) the 129 25-bp deletion variant (2) in exon 6 that results in the introduction of a premature termination codon in exon 7; (*ii*) a termination codon in exon 8 introduced by homologous recombination; and (*iii*) a polyadenylation signal in intron 8 introduced by homologous recombination, which results in the generation of a polyadenylated truncated transcript (2). The modifications in the *Disc1* allele are indicated by red arrows. (*B*) Western blot analysis of brain homogenates from WT and mutant *Disc1* mice. (*Left*) The ≈98-kDa band, corresponding to the predicted full-length proteins (L and L_v forms, http://genome.ucsc.edu) is undetectable in early postnatal day 2 brain lysates from HOM mutant *Disc1* mice (top red arrowhead) analyzed with the N-terminal antibody. The same band is reduced by about half in HET mutant mice. A band consistent with the predicted C-terminally truncated protein product (58 kDa) (black arrowhead) is detectable in lysates from HET and HOM mutant *Disc1* mice, but not WT littermates. This band is weak, indicating that the truncated protein missing the C-terminal portion is relatively unstable. Detection of this product proves unequivocally the specificity of our antibody. A ≈70-kDa band (bottom red arrowhead) is undetectable in HOM mutant *Disc1* mice and reduced by half in HET mutant *Disc1* mice. Two other weak low molecular weight bands appear unaffected by the mutation and may represent shorter N-terminal isoforms (2) (terminating before exon 6) or nonspecific signals (asterisks). Such short (putative) isoforms are expected to be produced and persist in the brains of the affected members of the Scottish family. (*Center*) Analysis with a C-terminal antibody. Red arrowheads indicate the major Disc1 isoforms at ≈98 and 70 kDa, which are missing in HOM mice. As predicted, no truncated protein is detected with this antibody. Asterisks indicate likely nonspecific cross-reactivity. (*Right*) Western blot of adult HPC lysates probed with the N-terminal antibody.

reliability of these antibodies when probing the pattern of expression of Disc1 isoforms (16) (M. Kvajo, unpublished work). Overall, the genetic lesion introduced into the endogenous *Disc1* orthologue models closely the Scottish mutation by virtue of the position of the introduced truncating lesions (in the vicinity of the translocation breakpoint) and of the fact that it preserves short N-terminal isoforms of the gene (http://genome.ucsc.edu). We used this mouse strain to examine in more detail two brain regions (HPC and mPFC) implicated in schizophrenia (17).

Morphological Analysis of the Adult mPFC. Low-resolution histology in Nissl-stained sections indicated no gross changes in HPC or mPFC morphology (Fig. S2 *A* and *C*). Volumetric analysis showed no genotypic differences in HPC volume ($P = 0.89$) (Fig. S2*B*), but revealed a small decrease (14%, $P < 0.05$) in PFC volume compared with WT littermate controls (Fig. S2*D*). By intercrossing mutant *Disc1* mice with a reporter strain (GFP-M) (18) we identified a ≈10% decrease ($P < 0.05$) in apical dendrite length of sparsely labeled layer V pyramidal neurons, which corresponds well with the decrease in the volume of this brain area (Fig. S2 *E* and *F*). We found no differences in the soma size or the mean angle of orientation (Fig. S2*F*). The complexity and total length of the basal dendritic tree and the apical tuft (Fig. S2 *G–J* and data not shown) were also unchanged, suggesting that the impaired extension of the apical dendrite may be caused by noncell autonomous restrictions imposed by the reduced mPFC volume. Finally, we found no differences in the numbers of calbindin- or parvalbumin-positive interneurons (Fig. S3 *A* and *B*).

Cytoarchitectural Alterations in the Adult Dentate Gyrus (DG). Postnatally, *DISC1* expression persists primarily in the DG (15), a brain region with active neurogenesis during adulthood (19). We did not observe any gross changes in DG morphology, and volumetric analysis did not show a significant decrease in the volume of the DG granule cell layer (GCL) in mutant *Disc1* mice ($P = 0.16$) (Fig. S4 *A* and *B*). In addition, immunocytochemistry with a calbindin antibody did not reveal any gross abnormalities in the mossy fiber tract (Fig. S4*A*).

Immature Granule Cells. In an effort to search for subtler morphological alterations, we first examined the immature neuronal population in the DG by using doublecortin (DCX) immunoreactivity. The subgranular zone (SGZ) of the DG harbors progenitor cells that continuously divide and give birth to new neurons, which migrate into the GCL, extend dendrites, and become integrated into functional circuits (19). In both genotypes, the majority of DCX-positive neurons were found in the SGZ and inner GCL with only a smaller proportion reaching the deeper layers of the GCL (Fig. 2*A*). However, a higher portion of cells was located in the outer layers of the GCL in mutant *Disc1* mice (Fig. 2*A*, arrows). Analysis of the distribution of the distance traveled by the furthest migrating cells (20) revealed that a larger fraction of these cells reached the outer layers of the GCL in mutant *Disc1* mice ($P = 0.024$) (Fig. 2*B*). The maturation of newly born neurons is tightly coupled to their migration, with more mature neurons occupying the outer layers of the GCL (21). No genotypic difference was observed in the number of DCX-positive cells expressing NeuN, a marker of mature neurons, suggesting that the ectopic localization is not a consequence of enhanced maturation (Fig. S4*C*).

The apical dendrites of most WT DCX-positive cells migrating into the GCL are oriented approximately perpendicular to the SGZ surface. By contrast, apical dendrites in mutant *Disc1* mice were often misoriented (Fig. 2*C*). To quantify this phenotype we measured the direction of each apical dendrite as an angle of orientation (θ) relative to the SGZ surface (22) (Fig. 2*D*). In WT mice, the mean angle of orientation was ≈10° (9.93 ± 1.43, $n = 42$ cells), whereas in mutant *Disc1* mice it was twice as large (19.08 ± 2.22, $n = 44$ cells, $P < 0.005$) (Fig. 2*E*). In WT mice, ≈7% of tested young neurons had apical dendrites projecting outside of the normal WT θ range (± 1.5 SD of the mean θ), whereas in mutant *Disc1* mice there was a marked increase in the number of neurons with apical dendrites projecting outside of this range (≈32% of tested young neurons). In addition, cells from mutant *Disc1* mice displayed a wider range of orientation angles with no correlation between migration distance and θ (data not shown).

During maturation, granule cells experience a sequence of morphological rearrangements, starting with cell morphotypes typified by a single, well delineated primary dendrite and ending with a characteristic morphotype with multiple primary branches extending directly from the cell soma (23). In both mutant and WT mice, the vast majority of immature granule cells extended only one primary apical dendrite with no apparent genotypic differences in the fraction of morphotypes (data not shown). Analysis of their dendritic tree revealed a small, nonsignificant trend toward a decrease in apical dendritic branchpoints and dendritic length in mutant mice ($P = 0.098$) (Fig. S4*D*). In addition, no genotypic differences were observed in soma size (data not shown).

Finally, we examined whether the observed alterations in the spatial distribution and orientation are accompanied by alter-

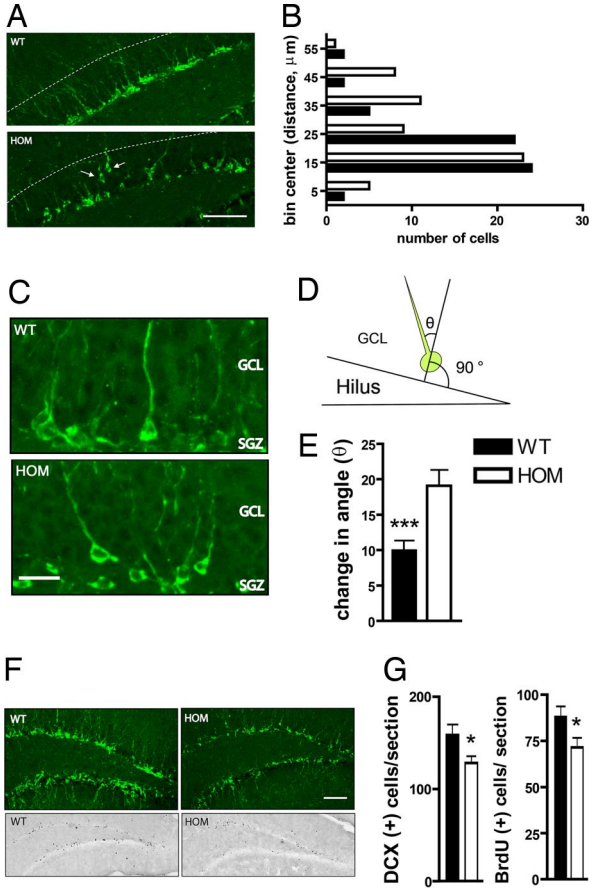

Fig. 2. Altered positioning and numbers of immature neurons. (*A* and *B*) Distribution of immature neurons in the GCL. (*A*) Representative images of DCX-positive neurons from HOM mutant *Disc1* mice and their WT littermates. Note the presence of DCX-positive neurons in the deeper layer of the GCL (arrows) of mutant mice. The dotted line represents the outer edge of the GCL. (*B*) Quantification of neuronal distribution performed by using the χ^2 test in a contingency analysis. $n = 54$ cells were analyzed for each genotype. (*C–E*) Dendritic orientation of immature neurons. (*C*) Representative images of DCX-positive neurons from HOM mutant *Disc1* mice and their WT littermates. (*D* and *E*) Quantification was performed by defining the angle of orientation (θ) for each apical dendrite (*D*) and calculating the mean change in θ (*E*). (*F* and *G*) Quantification of proliferating cells in the CGL. (*F*) Representative images of DCX-positive immature neurons (*Upper*) and BrdU-labeled neural precursor cells (*Lower*) in the DG of HOM mutant *Disc1* mice as compared with their WT littermates. (*G*) Quantification of DCX-positive immature neurons (*Left*) and BrdU-labeled neural precursor cells (*Right*). Values represent mean ± SEM. *, $P < 0.05$; ***, $P < 0.0001$. (Scale bars: *A* and *F*, 100 μm; *C*, 25 μm.)

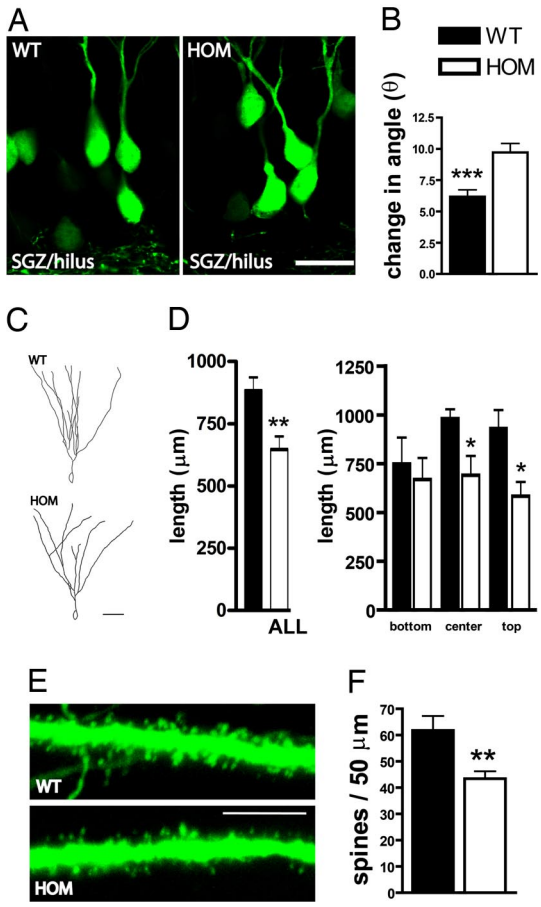

Fig. 3. Cytoarchitectural alterations in mature granule cells. (*A* and *B*) Dendritic orientation of DG granule cells. (*A*) Representative images of GFP-labeled mature granule cells. (*B*) Quantification of dendritic misorientation. (*C* and *D*) Dendritic length of DG granule cells. (*C*) Representative tracings of GFP-labeled mature granule cells. (*D*) Quantification of total dendritic length plotted against their position in the GCL. WT/HOM (*n*): all (14/17); top (4/6); center (6/7); bottom (4/4). (*E* and *F*) Dendritic spine density of DG granule cells. Representative images of dendritic spines (*E*) and quantification of their numbers (*F*). Values represent mean ± SEM. *, $P < 0.05$; **, $P < 0.001$; ***, $P < 0.0001$. (Scale bars: *A*, 25 μm; *C*, 50 μm; *E*, 5 μm.)

ation in the numbers of immature neurons. We found that in mutant *Disc1* mice the number of DCX-positive neurons per section is reduced by ≈19% [WT: 158.5 ± 11.36 ($n = 8$); mutant *Disc1*: 128.3 ± 7.4 ($n = 8$), $P < 0.05$] (Fig. 2 *F Upper* and *G*). To corroborate this finding, we injected mutant *Disc1* mice for 12 days with the thymidine analog BrdU to label the dividing cell population. Relative to WT littermates, mutant *Disc1* mice showed a 20% reduction in BrdU-labeled cells in the DG [WT: 87.94 ± 5.7 ($n = 10$); mutant *Disc1*: 71.45 ± 5.2 ($n = 8$), $P < 0.05$] (Fig. 2 *F Lower* and *G*). Quantification of the numbers of BrdU-labeled cells in the molecular layer revealed no genotypic differences, suggesting that the decreased numbers of BrdU-positive cells in GCL is not a consequence of abnormal migration and misplacement of a subset of cells outside of the GCL (data not shown).

Mature Granule Cells. We also analyzed GFP-expressing granule cells in mutant *Disc1* mice crossed to the Thy1-GFP reporter strain. The Thy-1 promoter directs expression in postmitotic neurons (24) and, as expected, the vast majority of GFP-expressing cells represent mature neurons that do not express DCX (Fig. S4*E*). Overall, mature granule cells from mutant *Disc1* mice showed normal soma size and there was no genotypic difference in the percentage of cells with one or more multiple dendrites (Fig. S4 *F* and *G*). Restricting our analysis to granule cells with a single, well delineated apical dendrite, we found that in WT mice the mean θ was ≈6° (6.176 ± 0.55, $n = 120$ cells), whereas in mutant *Disc1* mice it was increased by ≈40% (9.722 ± 0.7163, $n = 120$ cells, $P < 0.0001$) (Fig. 3 *A* and *B*). In WT mice, ≈10% of granule cells had apical dendrites projecting outside of the normal WT θ range (±1.5 SD of the mean θ), whereas in mutant *Disc1* mice this percentage increased to ≈22%. Thus, the misorientation phenotype is also present, albeit to a smaller degree, in mature granule cells.

Further analysis of dendritic complexity of GFP-expressing granule cells with a single apical dendrite revealed a 25% decrease in total dendritic length in mutant mice [WT: 882.6 ± 53.83 ($n = 14$ neurons); mutant *Disc1*: 645.8 ± 53.24 ($n = 16$ neurons), $P = 0.0042$] (Fig. 3 *C* and *D*). Interestingly, this decrease was evident in neurons located in the upper two-thirds

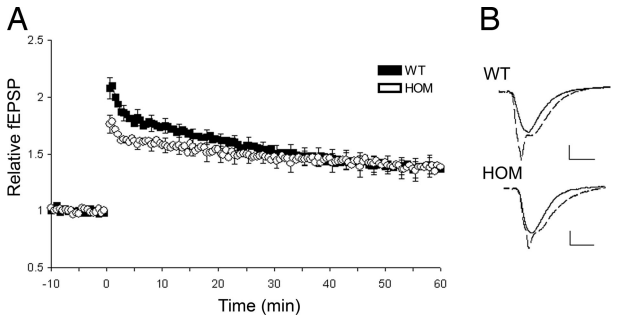

Fig. 4. Synaptic transmission and plasticity. (*A*) LTP in WT ($n = 17, 7$) and HOM ($n = 10, 6$) mice. There was a significant difference in the degree of potentiation of fEPSPs over time (min) (two-way repeated measures ANOVA; $P < 0.05$). Posthoc testing showed that 14 min immediately after tetanization the magnitude of potentiation in the HOM mutant *Disc1* mice was significantly lower than in WT controls. By contrast, the degree of LTP observed was unaffected by the mutation 1 h after tetanization. (*B*) Example traces of field EPSPs show responses before (solid line) and immediately after (interrupted line) tetanization.

of the GCL (top: $P = 0.04$, center: $P = 0.029$), but not in those found at the bottom part of the GCL (Fig. 3*D*). Because adult-born neurons are thought to contribute mainly to the inner layers of the DG (25), the lack of an effect in the bottom layer is consistent with our observation of near-normal dendritic growth in newly born neurons and suggests that impaired *Disc1* function specifically leads to a halting of dendritic growth during the postnatal maturation of granule cells in the DG. Finally, our analysis revealed a significant decrease in the number of spines (per 50 μm) in mutant *Disc1* mice [WT: 61.80 ± 5.463 ($n = 3$ mice/5 neurons per mouse); mutant *Disc1*: 43.40 ± 2.828 ($n = 3$ mice/5 neurons per mouse), $P = 0.0057$) (Fig. 3 *E* and *F*).

Cytoarchitecture and Synaptic Transmission at the Adult CA1 Subfield. Analysis of dendritic orientation, complexity and spine density in GFP-labeled pyramidal cells in the CA1 region revealed no differences (Fig. S5 *A–F*). Thus, the observed cellular phenotypes appear to be largely restricted to the DG. Lack of overt cellular alterations at the CA1 subfield afforded us the opportunity to examine whether the *Disc1* mutation affects synaptic transmission and plasticity independently of any effect on neuronal morphology. The CA1/CA3 synapse was investigated by using field recordings in the stratum radiatum of CA1 while stimulating the Schaffer collaterals in acute transverse slices of the HPC. Under baseline conditions the strength of synaptic transmission was unaltered by the *Disc1* mutation (Fig. S5*G*). Also, the release probability, as inferred from the degree of paired-pulse facilitation, was unchanged (data not shown). Long-term potentiation (LTP) was also unaffected 1 h after tetanization (Fig. 4). However, short-term potentiation (STP; i.e., the increase in excitatory postsynaptic potential (EPSP) size that persists for ≈15 min after tetanization) was significantly reduced in mutant mice (Fig. 4 and Fig. S5*H*). Mechanistic distinctions between STP and LTP are not well defined, but STP is thought to critically depend on increased presynaptic release (26).

A Truncating Lesion in the Endogenous *Disc1* Predominantly Affects WM. To obtain insights into how the *DISC1* disease risk allele modeled in our mouse strain affects cognition, we performed a comprehensive evaluation of mutant *Disc1* mice by using an array of five cognitive tests. Traditionally, HPC-dependent tasks, such as contextual fear conditioning (Fig. 5*A*), novel object recognition (Fig. 5*B*), Morris water maze (Fig. 5*C*), and the win-shift version of the eight-arm radial maze (Fig. 5*D*), all failed to reveal robust changes in associative fear learning, recognition memory, reference memory and short-term memory, respectively (see *SI Text*).

To test the robustness of, and expand on, our earlier findings of WM deficits in the same mutant *Disc1* mice, we used a discrete trial, two-choice delayed nonmatch to position (DNMP) task. Because our initial findings indicated WM deficits in both heterozygous (HET) and homozygous (HOM) mutant mice we included both genotypes to replicate this earlier result. Although both the win-shift and two-choice DNMP tasks require the retention and utilization of new information to guide behavior, only the two-choice task requires this information be held online, updated, and actively maintained in the face of potential interference, thus placing greater demands on the executive compo-

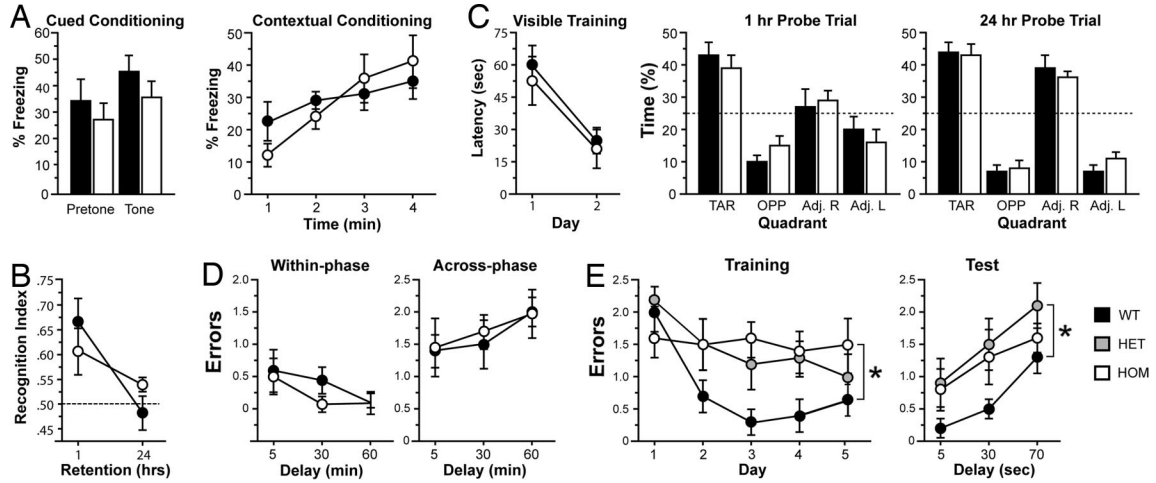

Fig. 5. A mutation in *Disc1* leads to specific pattern of cognitive deficits. (*A*) Fear conditioning. (*Left*) Conditioned freezing during the cued test ($n = 9$ WT, 9 HOM). Percent of time freezing during the 60 s before tone presentation (pretone) and during the 20-s tone presentation (tone). (*Right*) Percent time freezing during the 4 min of the contextual test. (*B*) Novel object recognition. Although the ability to recognize a familiar object significantly decreased with time, there were no differences between genotypes ($n = 9$ WT, 9 HOM). (*C*) Morris water maze. (*Left*) Latency to reach a visible platform did not differ between genotypes ($n = 9$ WT, 9 HOM). (*Center* and *Right*) Both genotypes spent more time in the target quadrant during the probe trials. (*D*) Win-shift task. Both genotypes made comparable numbers of within-phase (*Left*) and across-phase (*Right*) errors ($n = 9$ WT, 9 HOM). (*E*) Two-choice DNMP task. Both HET and HOM mutant *Disc1* mice made significantly more errors during training (*Left*) and testing (*Right*; $n = 10$ WT, 11 HET, 11 HOM). Values represent mean ± SEM. n.s., not significant; *, $P < 0.05$.

nents of WM (see *SI Text*). There was a main effect of training day indicating learning across days [$F_{(4, 116)} = 4.6$, $P = 0.0018$] and also a main effect of genotype [$F_{(2, 29)} = 4.2$, $P = 0.024$]. Both HOM and HET mutant *Disc1* mice showed a clear learning deficit compared with WT littermate controls and made more errors across training days (Fig. 5*E*; Dunnett's posthoc test, $P < 0.05$). Longer delays randomly introduced between the sample and choice phases increased errors [$F_{(2, 58)} = 11.2$, $P < 0.0001$], and again a main effect of genotype was found [$F_{(2, 29)} = 4.8$, $P = 0.015$] (Fig. 5*E Right*). Planned contrasts showed that both HOM and HET mutant mice made more errors than WT (Student's *t* test, $P < 0.05$) with no difference between each other (Student's *t* test, $P = 0.18$). These results are not caused by nonspecific motivational or motor effects because response times and average trial completion times did not differ between genotypes (see *SI Text* and Fig. S6).

Discussion

One finding of this study is the strong regional selectivity of the observed morphological alterations in HPC and mPFC. This pattern could be related to the intrinsic properties of neurons or a cell type-specific contribution of *Disc1* during embryonic and postnatal development dictated, at least in part, by its expression pattern (15). The mechanism behind the cellular aberrations may be related to the putative role of Disc1 at the centrosome (7) or in controlling cAMP levels (5, 27–29), although we cannot exclude other, yet-unexplored pathways. Morphological disturbances consistent with dendritic misorientation or impaired dendritic growth have been described in schizophrenia, albeit inconsistently (30, 31), and a recent study provided preliminary evidence for impaired adult neurogenesis in individuals with schizophrenia (32).

Kamiya *et al.* (6) have shown that shRNA-mediated depletion of Disc1 in embryonic cortical neurons inhibited their migration and induced misorientation and shortening of primary dendrites. Our analysis failed to confirm a widespread inhibition of migration in the DG, but rather revealed evidence consistent with "enhanced" migration, perhaps reflecting decreased sensitivity to repulsive guidance cues. This discrepancy could be caused by the different methodologies used, but it could also represent two different facets of misinterpretation of positional cues caused by impaired *Disc1* function (33). In addition, in our model, both the dendritic misorientation and impaired growth phenotypes were restricted to DG neurons and not found in pyramidal cortical neurons. Although the reason for this difference is unclear, it is possible that such morphological deficits are of transient nature in some populations of neurons while they persist in others.

A more recent study using acute shRNA-mediated down-regulation of Disc1 in newly born DG cells has also independently reported mispositioning of young neurons in the GCL (34). However, unlike our study, in that study this phenotype was accompanied by enhanced dendritic growth and accelerated spine formation, which led the authors to speculate that *Disc1* down-regulation results in accelerated functional neuronal integration. Instead, our results suggest that the newly generated DG neurons in mutant *Disc1* mice may be actually compromised and possibly not able to integrate into DG functional circuits. This possibility appears to be supported by the additional observation that mature granule cells show impaired dendritic growth and reduced number of spines. These findings raise an important general issue pertaining to the information obtained by models based on shRNA-mediated approaches as opposed to models based on germ-line genetic lesions. They also highlight important differences between these approaches that have to do with the timing and magnitude of the genetic disruption and the unique induction of compensatory responses that could be activated in germ-line genetic lesions to buffer against developmental insults.

The other finding of our study is the pattern of the observed cognitive deficits. Cognitive analysis (the most comprehensive of a *Disc1* mouse model reported to date) assessing various forms of memory revealed a significant deficit in a WM task that depends on the robust and active maintenance of information within WM networks in the face of irrelevant and competing information (35). This result is consistent with our previous findings with the same mutant *Disc1* mice using another WM task (2) and two subsequent studies showing spatial WM deficits in other *Disc1* models (9, 10). Lack of deficits in HPC-dependent cognitive assays of reference, recognition, and associative memory are consistent with the observed normal synaptic transmission and long-term plasticity at CA1/CA3 synapses. However, given the rapidly expanding study of the DG role in cognition (36–38), future studies using additional behavioral paradigms and larger experimental groups may reveal that *Disc1* deficiency affects restricted aspects of HPC-dependent cognition. In fact, although WM-dependent learning and performance critically depends on the functional integrity of the mPFC in rodents, manipulations of DG also produces spatial WM deficits in some cognitive paradigms (37), indicating that impaired DG and mPFC function may be interacting to contribute to the observed cognitive profile. Overall, *Disc1* deficiency leads to robust and reliable deficits in WM tasks with high executive components, suggesting these deficits may relate to WM and executive dysfunction observed in psychosis (17).

Independent of the underlying mechanism, our results strongly suggest that a mutation of endogenous mouse *Disc1* that resembles closely the one observed in an affected family has highly selective effects on brain structure and function. These effects likely represent genuine links between this well defined *DISC1* risk allele and disease susceptibility.

Materials and Methods

Animals. Genetically engineered mutant *Disc1* mice contain the same *Disc1* mutation backcrossed in C57BL/6J, as described by Koike *et al.* (2). All analyses were performed with 2- to 5-month-old male littermates produced by mating of HET mice. All animal procedures were approved by the Columbia University Institutional Animal Care and Use Committee.

Analysis of Migration, Dendritic Orientation, and Complexity. Analysis was essentially done as described (20, 22). For the migration analysis (20), confocal images of the DG were taken, and for each image the distance between the furthest DCX-positive cell and the SGZ/hilus border was measured. The furthest migrating cell was assigned to one of six 10-μm bins along the vertical axis of the DG. To analyze the apical dendrite orientation, ImageJ software was used to define a line from the center of the soma through 50–75 μm of the dendrite. The angle (θ) by this line relative to a line from the soma perpendicular to the SGZ was expressed in degrees (22). The quantification of dendritic complexity of granule cells and pyramidal neurons was performed essentially as described (18). Detailed descriptions of the methods can be found in *SI Text*.

BrdU Labeling, Immunohistochemistry, and Quantification of BrdU- and DCX-Positive Cells. Analysis was performed as described (39). Mice were injected with BrdU (50 mg/kg) for 12 consecutive days. BrdU and DCX stainings were performed on every sixth section of the entire HPC.

Western Blotting. Whole brains from postnatal day 2 pups or hippocampi from adult mice were dissected out, homogenized, and analyzed by Western blotting. The following antibodies were used: purified N-terminal anti-Disc1 Ab (1:100), purified C-terminal anti-Disc1 Ab (1:100), anti-Disc1 Ab from Santa Cruz Biotechnology (N16; 1:500) and anti-Disc1 Ab from Zymed (ZMD.488; 1:500). Conditions used for immunohistochemistry are described in *SI Text*.

Behavioral Assays. Behavioral studies were carried out as described (38, 40–42) (see also *SI Text*) in three groups of male mice (2–5 months old). Group 1 underwent training in the Morris water maze followed by the win-shift version of the radial arm maze and the novel object recognition test. Group 2

was subjected to fear conditioning test. Group 3 performed the two-choice DNMP task.

ACKNOWLEDGMENTS. We thank Dr. Michael Drew for assistance with behavioral tests and analyses and Amanda Garçia-Williams for management of the mouse colony. A portion of the behavioral phenotyping used the facilities of the Rodent Models Neurobehavioral Testing Core of the Lieber Center for Schizophrenia Research at Columbia University and the New York State Psychiatric Institute. This work was supported in part by National Institutes of Health Grants MH67068 (to M. Karayiorgou and J.A.G.) and MH77235 and MH080234 (to J.A.G.). H. McKellar is funded by National Institutes of Health Training Grant T32GM008224.

1. Millar JK, *et al.* (2000) Disruption of two novel genes by a translocation cosegregating with schizophrenia. *Hum Mol Genet* 9:1415–1423.
2. Koike H, Arguello PA, Kvajo M, Karayiorgou M, Gogos JA (2006) Disc1 is mutated in the 129S6/SvEv strain and modulates working memory in mice. *Proc Natl Acad Sci USA* 103:3693–3697.
3. Arguello PA, Gogos JA (2006) Modeling madness in mice: One piece at a time. *Neuron* 52:179–196.
4. Gogos JA, Gerber DJ (2006) Schizophrenia susceptibility genes: Emergence of positional candidates and future directions. *Trends Pharmacol Sci* 27:226–233.
5. Millar JK, *et al.* (2005) DISC1 and PDE4B are interacting genetic factors in schizophrenia that regulate cAMP signaling. *Science* 310:1187–1191.
6. Kamiya A, *et al.* (2005) A schizophrenia-associated mutation of DISC1 perturbs cerebral cortex development. *Nat Cell Biol* 7:1167–1178.
7. Morris JA, Kandpal G, Ma L, Austin CP (2003) DISC1 (Disrupted-In-Schizophrenia 1) is a centrosome-associated protein that interacts with MAP1A, MIPT3, ATF4/5, and NUDEL: Regulation and loss of interaction with mutation. *Hum Mol Genet* 12:1591–1608.
8. Hikida T, *et al.* (2007) Dominant-negative DISC1 transgenic mice display schizophrenia-associated phenotypes detected by measures translatable to humans. *Proc Natl Acad Sci USA* 104:14501–14506.
9. Clapcote SJ, *et al.* (2007) Behavioral phenotypes of Disc1 missense mutations in mice. *Neuron* 54:387–402.
10. Li W, *et al.* (2007) Specific developmental disruption of disrupted-in-schizophrenia-1 function results in schizophrenia-related phenotypes in mice. *Proc Natl Acad Sci USA* 104:18280–18285.
11. Pletnikov MV, *et al.* (2008) Inducible expression of mutant human DISC1 in mice is associated with brain and behavioral abnormalities reminiscent of schizophrenia. *Mol Psychiatry* 13:173–186.
12. Paterlini M, *et al*. (2005) Transcriptional and behavioral interaction between 22q11.2 orthologs modulates schizophrenia-related phenotypes in mice. *Nat Neurosci* 8:1586–1594.
13. Tabuchi K, *et al.* (2007) A neuroligin-3 mutation implicated in autism increases inhibitory synaptic transmission in mice. *Science* 318:71–76.
14. Bord L, *et al.* (2006) Primate disrupted-in-schizophrenia-1 (DISC1): High divergence of a gene for major mental illnesses in recent evolutionary history. *Neurosci Res* 56:286–293.
15. Austin CP, Ky B, Ma L, Morris JA, Shughrue PJ (2004) Expression of Disrupted-In-Schizophrenia-1, a schizophrenia-associated gene, is prominent in the mouse hippocampus throughout brain development. *Neuroscience* 124:3–10.
16. Ishizuka K, *et al.* (2007) Evidence that many of the DISC1 isoforms in C57BL/6J mice are also expressed in 129S6/SvEv mice. *Mol Psychiatry* 12:897–899.
17. Barch DM (2005) The cognitive neuroscience of schizophrenia. *Annu Rev Clin Psychol* 1:321–353.
18. Feng G, *et al.* (2000) Imaging neuronal subsets in transgenic mice expressing multiple spectral variants of GFP. *Neuron* 28:41–51.
19. Kempermann G, Wiskott L, Gage FH (2004) Functional significance of adult neurogenesis. *Curr Opin Neurobiol* 14:186–191.
20. Lazic SE, *et al.* (2006) Neurogenesis in the R6/1 transgenic mouse model of Huntington's disease: Effects of environmental enrichment. *Eur J Neurosci* 23:1829–1838.
21. Shapiro LA, Ribak CE (2005) Integration of newly born dentate granule cells into adult brains: Hypotheses based on normal and epileptic rodents. *Brain Res Brain Res Rev* 48:43–56.
22. Demyanenko GP, *et al.* (2004) Close homolog of L1 modulates area-specific neuronal positioning and dendrite orientation in the cerebral cortex. *Neuron* 44:423–437.
23. Wang S, Scott BW, Wojtowicz JM (2000) Heterogenous properties of dentate granule neurons in the adult rat. *J Neurobiol* 42:248–257.
24. Tiveron MC, *et al.* (1992) Selective inhibition of neurite outgrowth on mature astrocytes by Thy-1 glycoprotein. *Nature* 355:745–748.
25. Kempermann G, Gast D, Kronenberg G, Yamaguchi M, Gage FH (2003) Early determination and long-term persistence of adult-generated new neurons in the hippocampus of mice. *Development* 130:391–399.
26. Lauri SE, *et al.* (2007) Presynaptic mechanisms involved in the expression of STP and LTP at CA1 synapses in the hippocampus. *Neuropharmacology* 52:1–11.
27. Nakagawa S, *et al.* (2002) Regulation of neurogenesis in adult mouse hippocampus by cAMP and the cAMP response element-binding protein. *J Neurosci* 22:3673–3682.
28. Fujioka T, Fujioka A, Duman RS (2004) Activation of cAMP signaling facilitates the morphological maturation of newborn neurons in adult hippocampus. *J Neurosci* 24:319–328.
29. Song HJ, Ming GL, Poo MM (1997) cAMP-induced switching in turning direction of nerve growth cones. *Nature* 388:275–279.
30. Christison GW, Casanova MF, Weinberger DR, Rawlings R, Kleinman JE (1989) A quantitative investigation of hippocampal pyramidal cell size, shape, and variability of orientation in schizophrenia. *Arch Gen Psychiatry* 46:1027–1032.
31. Arnold SE, *et al.* (1995) Smaller neuron size in schizophrenia in hippocampal subfields that mediate cortical-hippocampal interactions. *Am J Psychiatry* 152:738–748.
32. Reif A, *et al.* (2006) Neural stem cell proliferation is decreased in schizophrenia, but not in depression. *Mol Psychiatry* 11:514–522.
33. Ayala R, Shu T, Tsai LH (2007) Trekking across the brain: The journey of neuronal migration. *Cell* 128:29–43.
34. Duan X, *et al.* (2007) Disrupted-In-Schizophrenia 1 regulates integration of newly generated neurons in the adult brain. *Cell* 130:1146–1158.
35. Touzani K, Puthanveettil SV, Kandel ER (2007) Consolidation of learning strategies during spatial working memory task requires protein synthesis in the prefrontal cortex. *Proc Natl Acad Sci USA* 104:5632–5637.
36. Niewoehner B, *et al.* (2007) Impaired spatial working memory but spared spatial reference memory following functional loss of NMDA receptors in the dentate gyrus. *Eur J Neurosci* 25:837–846.
37. McHugh TJ, *et al.* (2007) Dentate gyrus NMDA receptors mediate rapid pattern separation in the hippocampal network. *Science* 317:94–99.
38. Saxe MD, *et al.* (2006) Ablation of hippocampal neurogenesis impairs contextual fear conditioning and synaptic plasticity in the dentate gyrus. *Proc Natl Acad Sci USA* 103:17501–17506.
39. Meshi D, *et al.* (2006) Hippocampal neurogenesis is not required for behavioral effects of environmental enrichment. *Nat Neurosci* 9:729–731.
40. de Bruin JP, Moita MP, de Brabander HM, Joosten RN (2001) Place and response learning of rats in a Morris water maze: Differential effects of fimbria fornix and medial prefrontal cortex lesions. *Neurobiol Learn Mem* 75:164–178.
41. Floresco SB, Seamans JK, Phillips AG (1997) Selective roles for hippocampal, prefrontal cortical, and ventral striatal circuits in radial-arm maze tasks with or without a delay. *J Neurosci* 17:1880–1890.
42. Hammond RS, Tull LE, Stackman RW (2004) On the delay-dependent involvement of the hippocampus in object recognition memory. *Neurobiol Learn Mem* 82:26–34.